





## ORIGINAL ARTICLE

# Phytopathogenic bacteria utilize host glucose as a signal to stimulate virulence through LuxR homologues

Siyuan Zhang<sup>1,2</sup> | Jinhong Kan<sup>1,2</sup> | Xin Liu<sup>3</sup> | Yao Wu<sup>1</sup> | Mingyang Zhang<sup>1</sup> |  
Jinqing Ou<sup>1,2</sup> | Juan Wang<sup>1</sup> | Lin An<sup>1</sup> | Defeng Li<sup>1</sup> | Li Wang<sup>1</sup>  | Xiu-Jie Wang<sup>3</sup>  |  
Rongxiang Fang<sup>1</sup>  | Yantao Jia<sup>1</sup> 

<sup>1</sup>State Key Laboratory of Plant Genomics, Institute of Microbiology, Chinese Academy of Sciences, Beijing, China

<sup>2</sup>University of Chinese Academy of Sciences, Beijing, China

<sup>3</sup>State Key Laboratory of Plant Genomics, Collaborative Innovation Center of Genetics and Development, Institute of Genetics and Developmental Biology, Chinese Academy of Sciences, Beijing, China

## Correspondence

Yantao Jia, State Key Laboratory of Plant Genomics, Institute of Microbiology, Chinese Academy of Sciences, No. 1 Beichen West Road, Chaoyang District, Beijing 100101, China.  
Email: [jiayt@im.ac.cn](mailto:jiayt@im.ac.cn)

## Present address

Jinhong Kan, Institute of Crop Sciences, Chinese Academy of Agricultural Sciences (CAAS), Beijing, China

## Funding information

Strategic Priority Research Program of the Chinese Academy of Sciences, Grant/Award Number: XDA28030000; National Natural Science Foundation of China, Grant/Award Number: 31972233

## Abstract

Chemical signal-mediated biological communication is common within bacteria and between bacteria and their hosts. Many plant-associated bacteria respond to unknown plant compounds to regulate bacterial gene expression. However, the nature of the plant compounds that mediate such interkingdom communication and the underlying mechanisms remain poorly characterized. *Xanthomonas campestris* pv. *campestris* (Xcc) causes black rot disease on brassica vegetables. Xcc contains an orphan LuxR regulator (XccR) which senses a plant signal that was validated to be glucose by HPLC-MS. The glucose concentration increases in apoplast fluid after Xcc infection, which is caused by the enhanced activity of plant sugar transporters translocating sugar and cell-wall invertases releasing glucose from sucrose. XccR recruits glucose, but not fructose, sucrose, glucose 6-phosphate, and UDP-glucose, to activate *pip* expression. Deletion of the bacterial glucose transporter gene *sgIT* impaired pathogen virulence and *pip* expression. Structural prediction showed that the N-terminal domain of XccR forms an alternative pocket neighbouring the AHL-binding pocket for glucose docking. Substitution of three residues affecting structural stability abolished the ability of XccR to bind to the *luxXc* box in the *pip* promoter. Several other XccR homologues from plant-associated bacteria can also form stable complexes with glucose, indicating that glucose may function as a common signal molecule for pathogen-plant interactions. The conservation of a glucose/XccR/*pip*-like system in plant-associated bacteria suggests that some phytopathogens have evolved the ability to utilize host compounds as virulence signals, indicating that LuxRs mediate an interkingdom signalling circuit.

## KEYWORDS

glucose, interkingdom signalling, LuxR ligand, quorum sensing

Siyuan Zhang, Jinhong Kan, and Xin Liu contributed equally to this work.

This is an open access article under the terms of the [Creative Commons Attribution-NonCommercial-NoDerivs](https://creativecommons.org/licenses/by-nc-nd/4.0/) License, which permits use and distribution in any medium, provided the original work is properly cited, the use is non-commercial and no modifications or adaptations are made.

© 2023 The Authors. *Molecular Plant Pathology* published by British Society for Plant Pathology and John Wiley & Sons Ltd.

## 1 | INTRODUCTION

Communication mediated by low-molecular weight chemical signals between prokaryotes and eukaryotes, such as bacterial pathogens and their hosts, is known as interkingdom signalling (González & Venturi, 2013). To some extent, prokaryotes and eukaryotes form a regulatory network through exposure to the signalling molecules released by each other to activate new functions. Depending on the genetic pathways modulated by the communication signals, interkingdom signalling could be beneficial or harmful to both parties. It has been reported that plant-associated bacteria (PABs) have evolved the ability to monitor and respond to host-generated chemical signals, such as flavonoids, phenolic compounds, rosmarinic acid, L-cannavanine, and halogenated furanones, activating or suppressing the expression of specific bacterial genes (Brencic & Winans, 2005; Corral-Lugo et al., 2016; Keshavan et al., 2005; Manefield et al., 2002; Stachel et al., 1985; Vandeputte et al., 2010). One important chemical signalling mode is quorum sensing (QS) (Fuqua et al., 1994), which is typically used by bacteria for intraspecies or interspecies communication (Bassler et al., 1997; Miller & Bassler, 2001; Waters & Bassler, 2005), and even interkingdom signalling between eukaryotic hosts and microbes (Lowery et al., 2008; Shiner et al., 2005; Sperandio et al., 2011). N-acyl homoserine lactones (AHLs) produced by gram-negative bacteria are the most common group of bacterial QS signals, which bind to their cognate receptors (LuxRs), facilitating cooperative behaviour in cell populations (Fuqua et al., 2001). Several LuxR homologues of PABs respond to small diffusible plant compounds (González & Venturi, 2013). However, the molecules capable of inducing interkingdom signalling and their functional mechanisms remain poorly characterized.

The gram-negative phytopathogen *Xanthomonas campestris* pv. *campestris* (Xcc) is the causal agent of black rot of crucifers (Williams, 1980), such as cabbage and *Arabidopsis*. Unlike the well-studied AHL-QS system, Xcc only contains a *luxR* homologue gene, *XccR*, adjacent to *pip* (encoding a proline iminopeptidase), but lacks the AHL synthase gene *luxI* (Zhang et al., 2007). Both *XccR* and *pip* are essential for Xcc virulence, and the expression of *pip* is activated by the transcription factor XccR through responding to unknown plant compounds rather than AHLs (Zhang et al., 2007). XccR binds to the *luxXc* box, an inverted-repeat DNA element in the *pip* promoter, inducing *pip* expression and enabling the bacterial evasion of host immunity (Zhang et al., 2007). Intriguingly, numerous sequenced proteobacterial genomes have more *LuxR* than *LuxI* homologues because they lack the cognate *LuxI* AHL synthase genes (Case et al., 2008). These unpaired QS *LuxR* proteins have been called orphans or solos, and generally consist of a typical modular structure having an AHL-binding domain at the N-terminus and a DNA-binding helix-turn-helix (HTH) domain at the C-terminus (Fuqua, 2006; Subramoni & Venturi, 2009). A subfamily of the *LuxR* solos lacks conserved amino acid residues in the AHL-binding domain, lost the capacity to bind to AHLs, and instead evolved the ability to respond to low-molecular weight compounds produced by plants rather than AHLs (Chatnaparat et al., 2012; Ferluga et al., 2007; Ferluga &

Venturi, 2009; Subramoni et al., 2011; Venturi & Fuqua, 2013; Zhang et al., 2007). This kind of *LuxR* in PABs includes Xcc. Interestingly, these *LuxR* homologous genes are always adjacent to the virulence-associated *pip* genes instead of *LuxI*s in many PABs (González & Venturi, 2013). OryR of *Xanthomonas oryzae* pv. *oryzae* (Xoo), an orthologue of XccR, can also sense unidentified chemicals from a rice extract (Ferluga et al., 2007; Ferluga & Venturi, 2009). XagR of *Xanthomonas axonopodis* pv. *glycines* (Xag) (Chatnaparat et al., 2012) and PsoR of *Pseudomonas* spp. (Subramoni et al., 2011) were reported to respond to cognate plant signals, although the signals have not been characterized. An increasing body of evidence indicates that *XccR/pip*-like loci are widespread among PABs, implying their importance for plant-microbe communications, which may present a novel type of interkingdom signalling (González & Venturi, 2013). Much research attention has been focused on characterization of the plant signals and exploration of the mechanisms underlying the signalling pathways.

In this study, we demonstrate that plant-produced glucose serves as a signal for *XccR/pip* regulation. Molecular docking shows that glucose is embedded into a novel sugar-binding pocket neighbouring the putative AHL pocket in the XccR autoinducer domain. The structure of the highly conserved sugar-binding pocket of several *LuxR* proteins generated by 3D homology models and their high affinity for glucose implied that glucose may be important for host-plant interaction. Xcc induced expression of the specific sugar transporter and cell-wall invertase activity in host plants, which resulted in glucose accumulation at the bacterial infection site. Our findings extend our knowledge about glucose; it can serve not only as a major carbon source for bacterial growth, but also as a signal to stimulate bacterial virulence gene expression, which enhances the ability of phytopathogens to deal with host plant immunity as well as bacterial survival. Understanding the chemical communication between plants and bacteria could help to design new strategies to control plant pathogen infection.

## 2 | RESULTS

### 2.1 | Glucose is identified as an XccR-responsive signal

We previously found that an unknown plant compound enhanced the binding of XccR, a QS *LuxR* family protein, to the *luxXc* box and resulted in the activation of downstream PIP virulence factor expression in Xcc (Wang et al., 2011; Zhang et al., 2007). To further identify the effective plant components, we used the electrophoretic mobility shift assay (EMSA) as a monitor system to detect the functional fractions from the compound mixture, and then purified the active compounds by high-performance liquid chromatography (HPLC). Cabbage leaves were harvested at 48 h after Xcc inoculation, frozen in liquid nitrogen, and pulverized, and the leaf powder was extracted with solvents of different polarity. We found that water-extracted solution promoted XccR-*luxXc* box binding, as determined by EMSA.

Then, 1 kg of liquid nitrogen-frozen cabbage leaves was ground, water-extracted, and filtered by ultrafiltration with a 1 kDa cut-off membrane. The eluate with molecular weight below 1 kDa was further fractionated by HPLC. Mass spectrometry and nuclear magnetic resonance (NMR) analyses showed that the active compounds contain a mixture of  $\alpha$ - and  $\beta$ -D-glucose (Figure S1a), for the chemical shift values agreed with those in the  $^1\text{H}$  NMR and  $^{13}\text{C}$  NMR spectra of the reference compounds (Gorin & Mazurek, 1975; Kosaka et al., 2015) (Figure S1b,c; Table S1). As  $\alpha$ - and  $\beta$ -D-glucose are two anomers naturally existing in equilibrium, for convenience, we hereafter refer to D-glucose as glucose. The glucose concentrations of Xcc infection sites were 2.7-fold and 2.3-fold higher than those in uninfected tissues of *Arabidopsis* or cabbage plants at 3 days postinoculation (dpi), respectively (Figure 1a,b). To verify the positive effect of glucose on the binding of XccR to the *luxXc* box, we added different concentrations of glucose to the EMSA reaction mixture. The results showed that the binding ability of XccR to the *luxXc* box was enhanced with the addition of glucose in a concentration-dependent manner (Figure 1c), indicating that glucose has a positive effect on the binding between XccR and the *cis*-element. Although the abundance of fructose was also increased at the Xcc infection sites (Figure 1a,b), fructose did not enhance the binding of XccR to the *luxXc* box, as well as sucrose and the glucose derivatives glucose 6-phosphate and UDP-glucose (Figure S2a–f). The synthetic chemical 2-deoxyglucose was used as a nonmetabolizable glucose analogue; its binding affinity to XccR was similar to that of glucose in the microscale thermophoresis (MST) assay (Figure S2f). In EMSA, 2-deoxyglucose also enhanced the binding of XccR to the *luxXc* box (Figure S2d).

## 2.2 | Exogenous addition of glucose enhances $\beta$ -glucuronidase activity driven by the *pip* promoter

Like many bacteria, Xcc preferentially utilizes available glucose from the environment but does not synthesize glucose de novo (Tang et al., 2005). We found that the endogenous glucose content and  $\beta$ -glucuronidase (GUS) activity driven by the *pip* promoter in Xcc 8008 (Xcc 8004/*pip*-GUS) (Zhang et al., 2007) were slightly increased with bacterial growth in minimal medium (MM) with 25 mM glucose (Figure S3). To investigate whether exogenous glucose affects GUS activity, we generated a glucose transporter *sglT* mutant strain ( $\Delta$ *sglT*) from Xcc 8008 (Chen et al., 2014). Overnight bacterial culture in NYG medium was transferred to MM with 25 mM glucose for an additional 10 h of culturing. As shown in Figure 2a,b, exogenous glucose led to an increase of bacterial cellular glucose content and GUS activity in Xcc 8008, whereas the cellular glucose content and GUS activity of the  $\Delta$ *sglT* mutant were significantly decreased relative to Xcc 8008 (Figure 2a,b). To further validate whether XccR binds to glucose in the cytoplasm, XccR was isolated from Xcc 8004 cultured in MM with 25 mM glucose. The remaining glucose content was measured after XccR isolation from the cell lysate. The results showed that XccR-bound glucose accounted for 35% of cytoplasmic

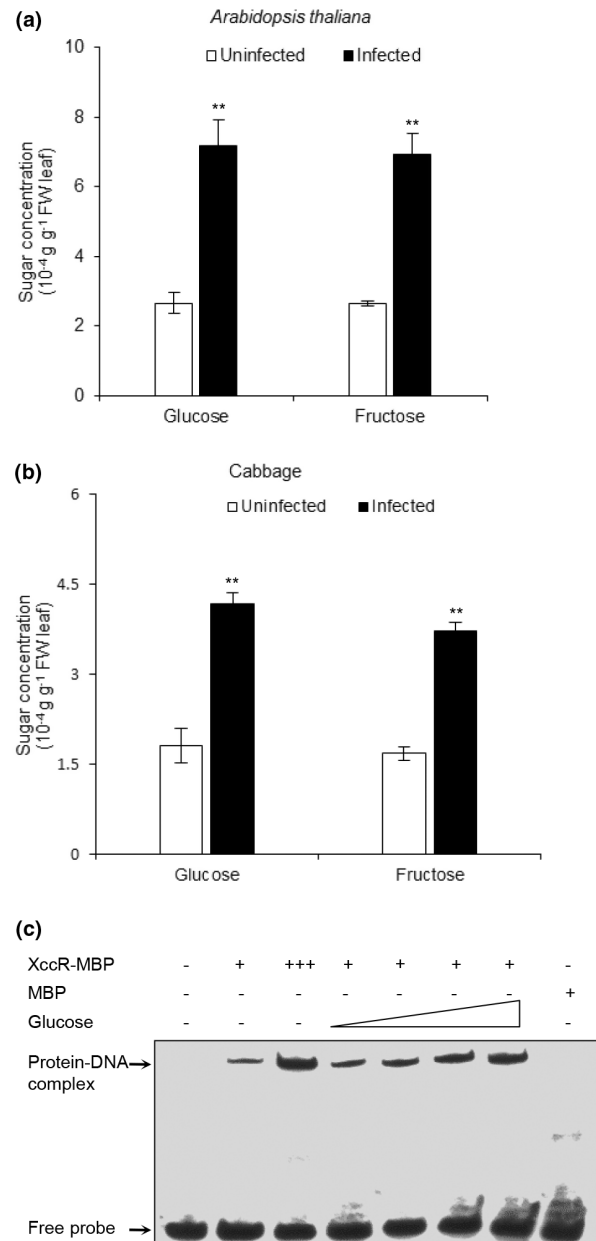


**FIGURE 1** *Xanthomonas campestris* pv. *campestris* (Xcc) infection induces sugar accumulation in host plants and glucose enhances XccR-DNA binding. (a and b) Accumulation of glucose and fructose in *Arabidopsis* (a) and cabbage (b) leaves after Xcc infection. FW, fresh weight;  $n = 4$ . Error bars represent SEM.  $**p < 0.001$ , two-tailed  $t$  test. (c) The binding ability of XccR to the target DNA sequence (the *luxXc* box) with increasing concentrations of glucose as determined by electrophoretic mobility shift assay. Each “+” represents 20 pmol XccR-MBP; the right triangle represents the addition of glucose with a gradient of 0.005, 0.05, 0.5, and 5  $\mu\text{M}$ . DNA probe is the [ $^{32}\text{P}$ ]-labelled *luxXc* box sequence. MBP, maltose-binding protein.

glucose (Figure 2d). These results indicated that XccR may recruit glucose from its niche and induce *pip* expression.

In order to study whether other sugar metabolites, such as UDP-glucose, participate in the regulation of *pip* expression by XccR, Xcc 8008 and  $\Delta$ *sglT* were incubated with 200  $\mu\text{M}$  2-deoxyglucose,

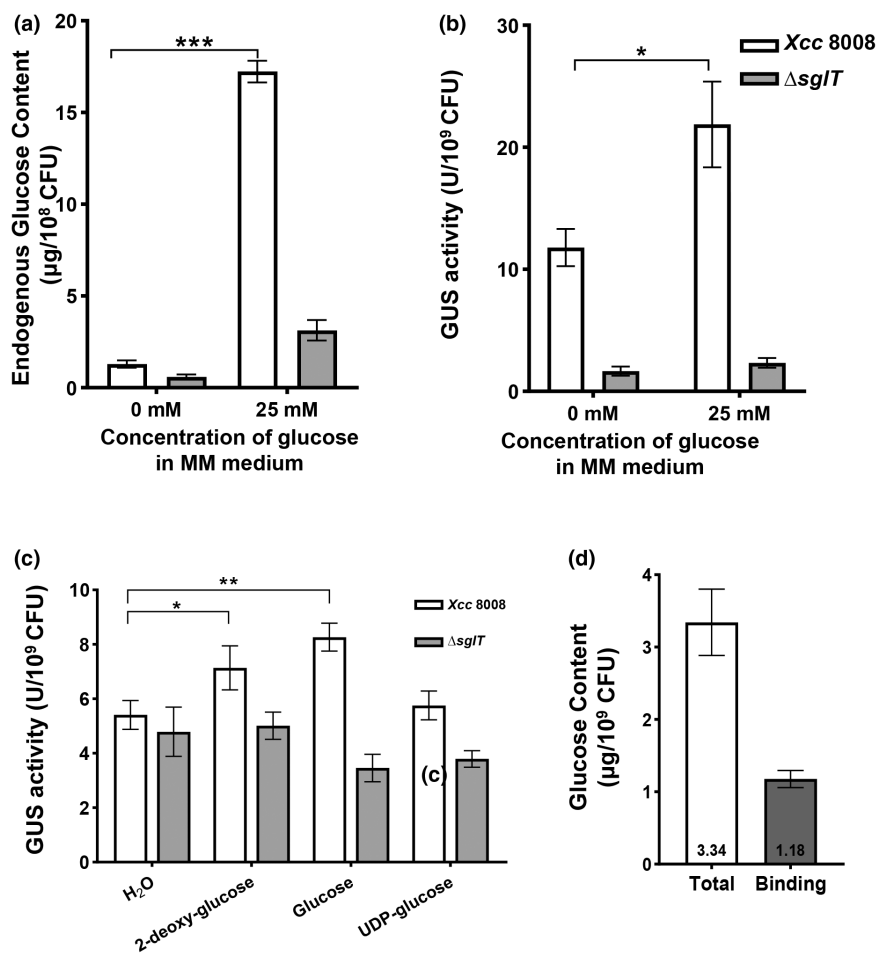


**FIGURE 2** Exogenous supply of glucose enhances *pip* expression. (a and b) Addition of 25 mM glucose in minimal medium (MM) increased the bacterial endogenous glucose content (a) and  $\beta$ -glucuronidase (GUS) activity in Xcc 8008 (b). (c) GUS activity in *Xanthomonas campestris* pv. *campestris* (Xcc) 8008 and  $\Delta sglT$  after 6 h of incubation with 200  $\mu\text{M}$  2-deoxyglucose, glucose, or UDP-glucose; water was used as a control. (d) The XccR-bound glucose content in Xcc 8004 cultured to  $\text{OD}_{600} = 0.3$  in MM with 25 mM glucose. \* $p < 0.05$ , \*\* $p < 0.001$ , \*\*\* $p < 0.0001$ , two-tailed t test. Error bars represent SEM.

glucose, or UDP-glucose for 6 h. The addition of 2-deoxyglucose and glucose, but not UDP-glucose, promoted GUS activity in Xcc 8008 (Figure 2c).

### 2.3 | XccR interacts with glucose through a novel predicted pocket

Similar to AHL-type LuxRs, XccR contains a putative N-terminal ligand-binding domain and a C-terminal DNA-binding domain (Zhang et al., 2007). To identify the cavity responsible for the interaction with the ligand, we performed in silico modelling based on existing LuxR crystal structures. Protein–ligand docking analysis revealed a new pocket, designated as a glucose-binding pocket here, within the N-terminal ligand-binding domain of XccR, which could stably harbour one molecule of glucose in one XccR monomer (Figure 3a). The glucose-binding pocket is formed by three  $\alpha$ -helices on the top of five antiparallel  $\beta$ -sheets (Figure 3a). Two residues (Cys21 and Tyr41) of XccR were predicted to form hydrogen bonds with glucose, and Gln60 of XccR forms hydrogen bonds with Cys21 and Tyr41 to stabilize their binding to glucose (Figure 3b). It is well known that the LuxR structures of the majority of gram-negative bacteria contain a pocket for AHLs (Waters & Bassler, 2005; Whitehead et al., 2001), yet Xcc and many other species of the *Xanthomonas* genus do not

harbour AHL synthesis genes (Cha et al., 1998), nor do they respond to AHLs synthesized by other bacteria (Zhang et al., 2007). Consistent with this fact, the newly predicted glucose-binding pocket of XccR is adjacent to the putative yet nonfunctional AHL-binding pocket; both are located in the N-terminal ligand-binding domain of XccR and are structurally separated by five antiparallel  $\beta$ -sheets. The existence of such an alternative glucose-binding pocket in XccR may extend the capability of Xcc to sense different signals, especially from host plants.

We further conducted MST (Panchal et al., 2016) and isothermal titration calorimetry (ITC) (Sperandio et al., 2011) experiments to examine the direct interaction between XccR and glucose in vitro. Both maltose-binding protein (MBP)-tagged and SUMO-tagged XccR could bind to glucose, showing similar  $K_d$  values of 251.69 nM and 241.61 nM, respectively (Figure 3c–e), supported by the ITC results, whereas neither the MBP tag nor the SUMO tag alone showed glucose-binding affinity (Figure 3c,e). In concert with the prediction results, mutating any or all residues within XccR (Cys21, Tyr41, and/or Gln60) reduced or abolished the binding ability of XccR to glucose in MST assays (Figure S4a–d). Furthermore, EMSA results showed that substitution of Tyr41 by alanine or triple mutation of the three residues abolished the binding ability of XccR to the *luxXc* box (Figure S4e), and mutating Cys21 or Gln60 to alanine reduced the protein–DNA binding affinity (Figure S4f,g). These results indicated

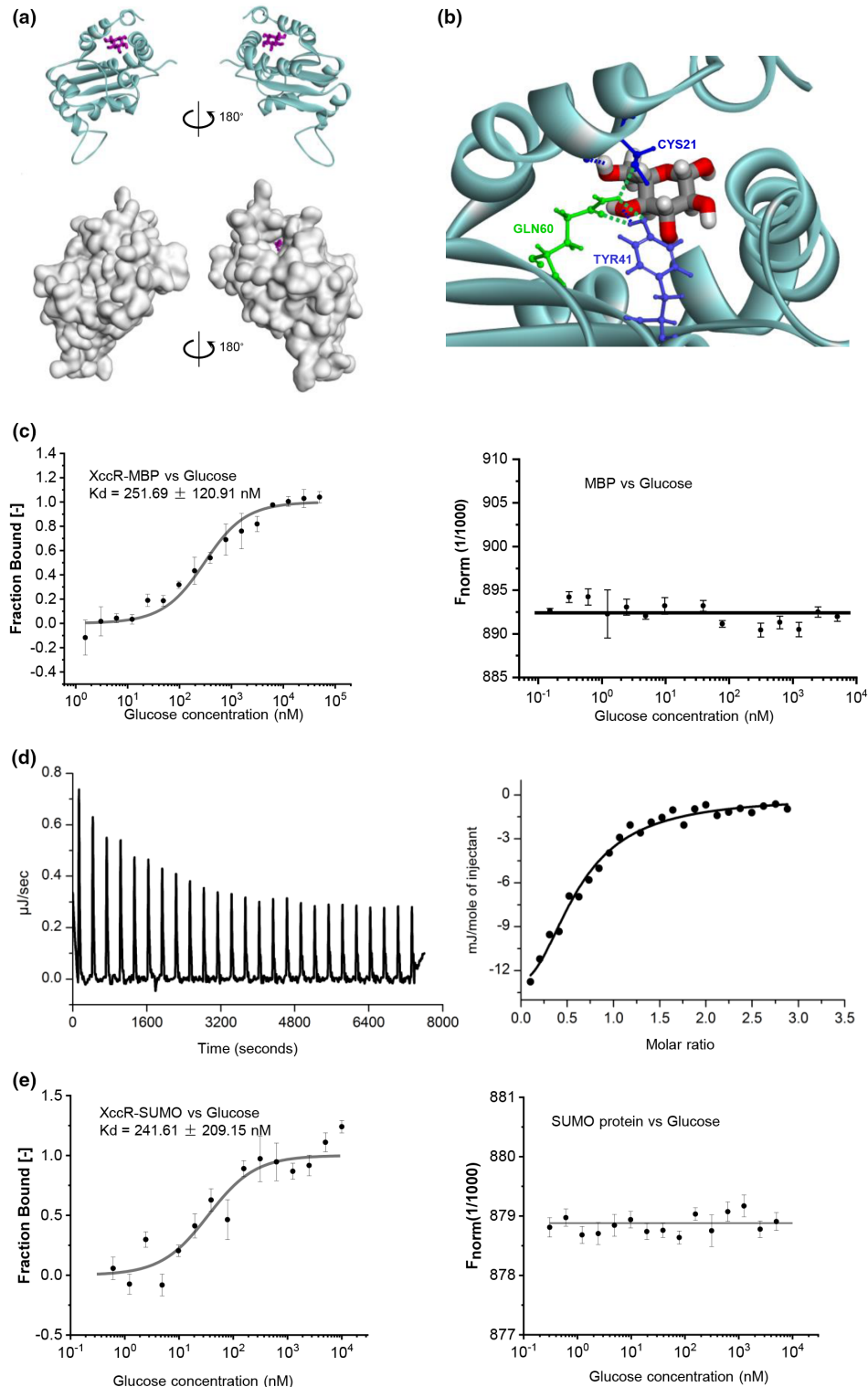


**FIGURE 3** XccR recruits glucose as a signal. (a) A docking model of XccR with glucose. The top panel shows glucose in purple and XccR in cyan. The bottom panel shows the solvent-accessible surface of XccR. (b) Essential residues of XccR for interaction with glucose. Amino acids forming hydrogen bonds with glucose (Cys21 and Tyr41) and the corresponding hydrogen bonds are shown as blue dashed lines; the amino acid (Gln60) forming hydrogen bonds with Cys21 and Tyr41 to stabilize the glucose-recognizing interface of XccR and the corresponding hydrogen bonds are shown as green dashed lines. (c) XccR-MBP binds glucose, as determined by microscale thermophoresis (MST) assays ( $n = 3$ ) with maltose-binding protein (MBP) as the negative control. Error bars represent SEM. (d and e) XccR-SUMO binds glucose, as determined by MST assays, with the SUMO protein as the negative control. Isothermal titration calorimetry assay detecting the binding of XccR with glucose. Results shown are for XccR-MBP (10  $\mu\text{M}$ ) titrates with 100  $\mu\text{M}$  glucose.

that glucose may help to sustain the structure of XccR suitable for binding to the *cis*-element of the downstream *pip* gene.

## 2.4 | Bacteria activate specific SWEETs and cell-wall invertases of *Arabidopsis*

The reallocation of carbohydrates to infection sites of leaf tissues is frequently observed in plants after invasion by viral, bacterial, and fungal pathogens (Berger et al., 2007). In most plants, sucrose is the major carbohydrate of such reallocation, which will be further hydrolysed into glucose and fructose by cell-wall invertases (Ruan, 2014). To examine whether the glucose distribution could be altered by Xcc in plant cells, we investigated the expression profiles of the SWEET family genes (encoding sugar efflux transporters) and cell-wall invertase activities at the infection sites. Among the 17 putative SWEET genes in *Arabidopsis thaliana*, only the *AtSWEET2* and *AtSWEET15* mRNA levels increased 4.3-fold and 51.5-fold at 36 h postinfection (hpi) by Xcc compared with the uninfected plants, respectively (Figure 4a). Disruption of these two *AtSWEET* genes resulted in a significant decrease of glucose accumulation in the apoplastic fluid of Xcc infection loci (Figure 4b) and led to a restriction of pathogen growth in the host plant leaves (Figure 4c,d), showing decreased bacterial numbers of Xcc in mutants defective in *AtSWEET2* (*Atsweet2-3-2* [SALK\_048430]) and *AtSWEET15* (*Atsweet15-4-7* [SALK\_031720]) relative to that of the wild-type plants. In addition, the enzymatic activity of cell-wall invertases was markedly increased in the apoplastic fluid isolated from Xcc-inoculated leaves (Figure S5a) in concert with the augmented glucose:sucrose molar ratio (1.5) (Figure S5b). Furthermore, the cell-wall invertase deficient mutants *cwinv1-2-1* (SALK\_091455) and *cwinv1-3-4* (SALK\_119499) were more resistant than wild-type plants at 3 dpi after being challenged with Xcc (Figure S5c). These findings showed that expression of both *AtSWEET* and *AtCWINV* was promoted to alter carbohydrate allocation upon pathogen infection.

Further tests were performed to determine if the induction of the virulence gene *pip* is a result of augmented binding of XccR to the *pip* promoter mediated by glucose. We compared the *pip* expression in wild-type (Col-0) and *Atsweet* mutant plants infected with the Xcc 8008 reporter strain (chromosomal expression of a *pip*-P/*gusA* chimeric gene in a wild-type Xcc 8004 background). As expected, the bacterial GUS (Lapin et al., 2019) activities driven by the *pip* promoter were decreased significantly in *Atsweet2-3-2* and *Atsweet15-4-7* mutant plants, but were restored to the wild-type level when the bacterial suspension was supplemented with glucose before infection (Figure 4e). In contrast, the *pip* expression level was quite low in rich medium or MM compared to in planta (Zhang et al., 2007). Deletion of XccR in the Xcc 8008 reporter strain impaired the GUS activity driven by the *pip* promoter in wild-type *Arabidopsis* plants, and such reduction could be complemented by plasmid-mediated overexpression of XccR (Figure 4f). However, mutating the residues required for glucose binding (Cys21, Tyr41, Gln60) in the XccR expression plasmid led to only partial restoration of GUS activity (Figure 4f),

suggesting that glucose is required for XccR-induced expression of *pip* and the abovementioned three residues are essential for XccR activity. Furthermore, deletion of the glucose transporter gene *sgIT* in the Xcc 8008 strain led to a decrease of GUS activity (Figure S6b) and bacterial virulence (Figure S6a), which could be restored by complementation, implying that glucose is required for *pip* expression.

## 2.5 | Several LuxR homologues also recruit glucose as a ligand

To investigate whether glucose could be utilized as a ligand by other PABs, we analysed the structures of several LuxR homologues in silico, including XagR (Q5E\_RS0113060) from Xag (Chatnaparat et al., 2012), OryR (PXO\_RS18575) from Xoo (Ferluga et al., 2007), PsoR (PFL\_RS26900) from *Pseudomonas fluorescens* (Subramoni et al., 2011), PsyR (PSPTO\_3863) from *Pseudomonas syringae* pv. *tomato* DC3000 (Pst DC3000) (Chatterjee et al., 2007), QscR (PA1898) from *Pseudomonas aeruginosa* PAO1 (Bottomley et al., 2007; Lintz et al., 2011), and LasR (PA1430) from *P. aeruginosa*, and also TraR (pTi\_029) from *Agrobacterium tumefaciens*, which is the first crystallized LuxR protein (Vannini et al., 2002; Zhang et al., 2002). A phylogenetic tree was constructed by MEGA 7 (Figure S7a). The glucose docking prediction results indicated that except for TraR and LasR, all other examined LuxRs contained the putative glucose-binding pocket and could form hydrogen bonds with glucose (Figure 5a–e, Figure S7c,d). Alignment of the amino acid sequences of the LuxRs showed that three residues, Cys21, Tyr41, and Gln60, were conserved among XccR, OryR, and XagR. The three residues contributed to the formation of hydrogen bonds for XccR to recognize glucose (Figure S7b). 3D structures of LuxRs exhibited structural homology, though the primary sequence of the LuxRs (excluding XccR, OryR, and XagR) had extremely low homology with each other (c.20%). These LuxRs were predicted to use different residues to form hydrogen bonds with glucose (Figure 5a–e). Consistent with the prediction results, the MST assays also verified that the LuxR homologues with higher Libdock scores showed higher binding affinity to glucose, but not sucrose and fructose, and vice versa (Figure 5a–e, Table S2). These data indicated that glucose may function as a signal ligand for LuxRs with the glucose-binding pocket in their structures. Among the identified glucose-binding LuxRs, five (XccR, OryR, XagR, PsoR, and QscR) are LuxR solos, as their original bacteria lack the adjacent AHL synthase genes in their genomes (Subramoni & Venturi, 2009).

## 3 | DISCUSSION

Plant–bacteria interkingdom signalling mediated by plant-derived glucose through the bacterial transcription factor XccR is summarized in a model shown in Figure 6. This work reports that glucose, which is dramatically induced in host plants by Xcc infection, functions as a signal sensed by XccR, indicating that Xcc is able to recruit host-produced chemical compounds for bacterial fitness. We found that

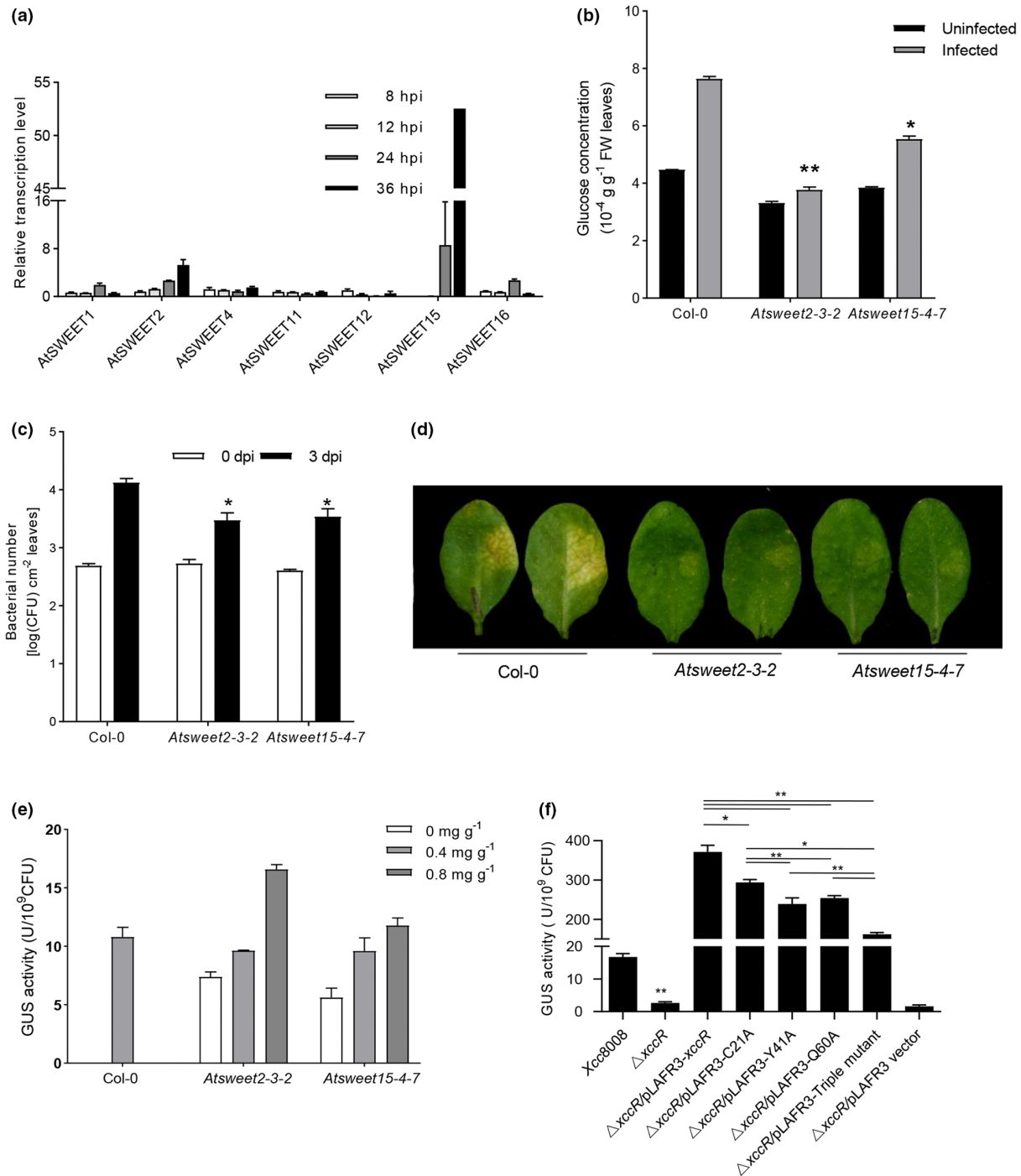


**FIGURE 4** AtSWEET2 and AtSWEET15 are required for sugar transportation after *Xanthomonas campestris* pv. *campestris* (Xcc) infection. (a) Relative expression levels of AtSWEET members in *Arabidopsis* leaves after Xcc infection. hpi, hours postinfection. (b) Xcc infection alters apoplastic glucose flux in wild-type *Arabidopsis* (Col-0) but not in AtSWEET2 or AtSWEET15 loss-of-function mutants (Atsweet2-3-2 or Atsweet15-4-7). FW, fresh weight;  $n = 5$ . (c and d) Reduced bacterial population (c) and virulence (d) of Xcc in AtSWEET2 or AtSWEET15 loss-of-function mutant leaves,  $n = 6$ . (e) Glucose restores *pip* promoter-driven  $\beta$ -glucuronidase (GUS) activities in Atsweet2 or Atsweet15 loss-of-function mutants,  $n = 3$ . (f) Effects of essential amino acids of XccR on *pip* expression. The *pip* promoter-driven GUS activities were detected after infiltration of bacteria into plants,  $n = 9$ . GUS activities were normalized to the bacterial population before comparison between samples. \* $p < 0.05$ , \*\* $p < 0.001$ , two-tailed t test. Error bars represent SEM. Scale bar in (d), 0.5 cm.

SWEET family sugar transporter expression and cell-wall invertase activity were induced during Xcc infection, which facilitated glucose accumulation in the apoplastic space. Opposite behaviour has

also been reported, as induction of SWEET expression by soilborne pathogen infection limits the carbon efflux from roots into the rhizosphere, rendering plants more resistant (Chen, Huh, et al., 2015).

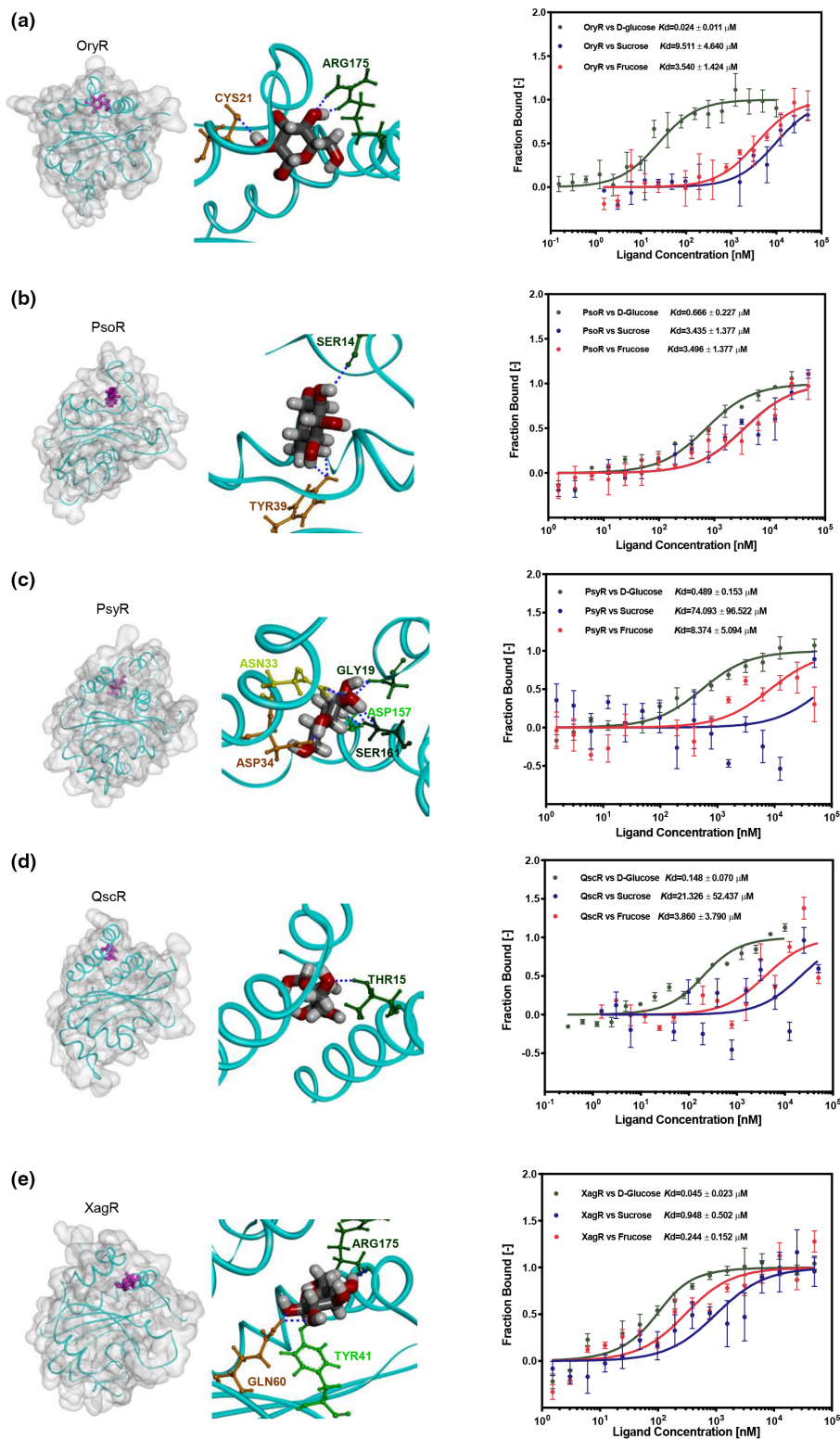


**FIGURE 5** Conservation of the glucose-binding pocket and glucose-binding ability in LuxR homologues of several plant-associated bacteria. (a–e) Glucose binding models of LuxR homologues: OryR (a), PsoR (b), PsyR (c), QscR (d), and XagR (e). Left, the presence of a predicted glucose-binding pocket in each protein. The hydrogen bonds between essential residues and glucose are shown as blue dashed lines. Right, the relative binding curves of LuxR-MBPs and sugars as determined by microscale thermophoresis assays.

The allocation of sugar made it possible for glucose to participate in the plant–microbe communication. In fact, the allocation of carbohydrate to pathogen infection sites by viruses, bacteria, and fungi is

frequently observed (Berger et al., 2007). Secretion of TAL effectors and activation of SWEET transporters by *Xanthomonas* species are found to be crucial for rice pathogen invasion (Chen et al., 2010; Yang



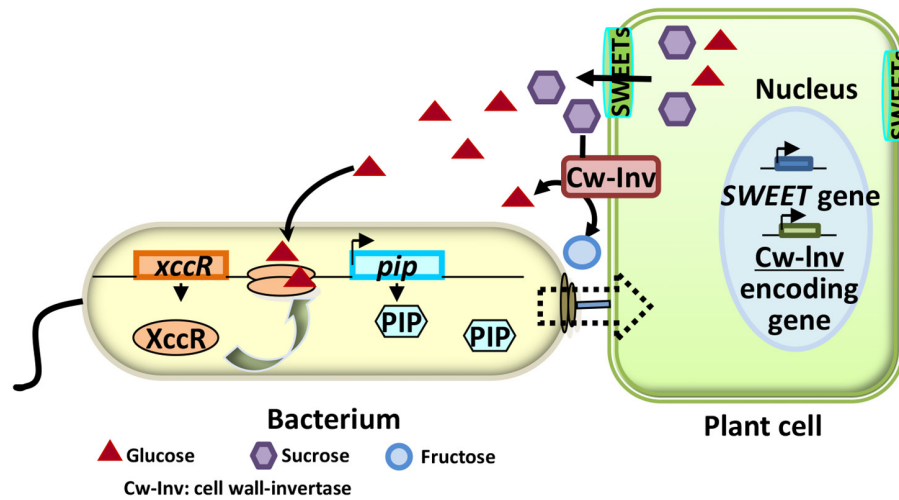


**FIGURE 6** Working model of glucose as a signal sensed by the bacterial transcription factor XccR. *Xanthomonas campestris* pv. *campestris* infection promotes the expression of host plant sugar transporters, which leads to sugar accumulation at the infection sites. The translocated sucrose is hydrolysed to glucose and fructose by cell-wall invertase (Cw-Inv). XccR senses and binds to glucose to induce expression of the virulence gene *pip*.

et al., 2006; Yu et al., 2011); however, how Xcc regulates SWEET gene expression remains unclear. Pathogens might take advantage of carbohydrate accumulation for disease development (Seo et al., 2007), whereas reprogramming and redirecting of carbon flow is also believed to support the successful establishment of resistance in plants, known as “high sugar resistance” (Horsfall & Dimond, 1957). Several lines of evidence show that in various plants, sucrose, but not glucose and fructose, specifically stimulates resistance gene expression (Yoon et al., 2021). Interestingly, our findings demonstrated that bacterial pathogens might recruit glucose as the signal for stimulating virulence gene expression, facilitating invasion and propagation. Hence, the final outcome of plant–pathogen interaction may to some extent depend on their ability to compete for sugars.

Like many bacteria, Xcc preferentially utilizes available glucose from the environment, but does not synthesize glucose *de novo* (Tang et al., 2005). In fact, many phytopathogens acquire glucose from their hosts and hijack host sugar efflux systems and cell-wall invertases to suppress host immunity (Kocal et al., 2008; Patrick, 1989; Ruan, 2014; Sutton et al., 1999; Voegele et al., 2001). We have elucidated that Xcc alters glucose flux through activating the expression of specific sugar transporter AtSWEET genes, AtSWEET2 and AtSWEET15 in *Arabidopsis*, whereas disruption of either of the two AtSWEETs led to reduced accumulation of glucose after being challenged by Xcc, resulting in restriction of bacterial growth and a decrease of XccR-mediated *pip* expression. Though AtSWEET family members have different cellular localizations (Chen et al., 2010; Eom et al., 2015; Yuan et al., 2014; Yuan & Wang, 2013), AtSWEET2 and AtSWEET15, which are located in the plasma membrane (Chen et al., 2010; Eom et al., 2015; Yuan et al., 2014; Yuan & Wang, 2013), are responsible for glucose and sucrose transport, respectively (Chen, Cheung, et al., 2015; Chen, Huh, et al., 2015). Another phytopathogen, Pst DC3000, activated the expression of AtSWEET15 and six other AtSWEETs in *Arabidopsis*. We found that the growth of Pst

DC3000 had no significant differences between the wild-type Col-0 and *Atsweet2* or *Atsweet15* mutant plants (Figure S8a,b), showing the functional redundancy of AtSWEETs induced by Pst DC3000, and the fold changes of glucose levels are similar between Col-0 and the mutant plants (Figure S8c). Though phytopathogens may use different strategies to hijack sugar transporters for bacterial infection, how these sugar transporters are switched on is still unknown.

On the plant apoplastic interface, sucrose can be hydrolysed by cell-wall invertases (Ruan, 2014). Among the six cell-wall invertase genes in *Arabidopsis*, *AtCWINV1* is strongly expressed in stems, leaves, and roots (Tymowska-Lalanne & Kreis, 1998). We found that the transcript level of *AtCWINV1* and the enzymatic activity of cell-wall invertase were induced by Xcc, resulted in a high ratio of glucose converted from sucrose in the apoplast fluid, which is consistent with previous reports (Bonfig et al., 2010; Fotopoulos et al., 2003). It is likely that sucrose transported by AtSWEETs can be converted to glucose by cell-wall invertases, resulting in elevated glucose levels at infection sites.

*LuxR* solos (or orphans), which are not genetically adjacent to *luxI*-like AHL synthase genes, are found in many bacteria (Fuqua, 2006; Subramoni et al., 2015; Subramoni & Venturi, 2009). Some *LuxR* solos in gram-negative bacteria can respond to self-produced AHLs or exogenous AHLs generated by bacteria of the same or a different species (Ahmer, 2004; Subramoni & Venturi, 2009). In this study, we found that one *LuxR* solo (XccR) of Xcc functions as a signal receptor recognizing plant-derived glucose rather than canonical QS signal AHLs (Zhang et al., 2007). XccR belongs to a special subgroup of *LuxR* solos from PABs, which respond to yet uncharacterized plant signal(s) (González & Venturi, 2013). Besides XccR, other members of this group include *OryR* of *Xoo* (Ferluga et al., 2007; Ferluga & Venturi, 2009), *XagR* of *Xag* (Chatnaparat et al., 2012), *QscR* of *P. aeruginosa* (Lintz et al., 2011), and *PsoR* of *P. fluorescens* (Subramoni et al., 2011). Our MST assay demonstrated that these *LuxR* solos

can also interact with glucose (Figure 5a,b,d,e). In addition, QscR was previously found to sense AHLs (Fuqua, 2006), indicating that the LuxR solo responds to at least two types of signalling molecules. This is also true for PsyR of Pst DC3000, which is not a LuxR solo, but functionally paired with a LuxI homologue (PsyI) (Chatterjee et al., 2007), and could recruit both AHL and glucose as binding ligands (Chatterjee et al., 2007) (Figure 5c). Our results implied that some, if not all, PABs with LuxR solos have evolved to adapt to host plant environments by recruiting crosskingdom signals, such as glucose. For PsyR and QscR from *Pseudomonas*, glucose acts as an additional communication signal, because the bacteria can synthesize and respond to AHLs as well (Chatterjee et al., 2007; Lee et al., 2006). Interestingly, one tested LuxR homologue, QscR from *P. aeruginosa* PAO1, can invade both plants and humans (Rahme et al., 2000); whether PAO1 also utilizes glucose to regulate its own gene expression in humans needs to be explored.

The canonical QS-AHL LuxRs and PAB LuxR solos all have an N-terminal ligand-binding domain (Shadel et al., 1990) and a C-terminal HTH DNA-binding domain (Choi & Greenberg, 1991, 1992). We predicted a novel pocket for glucose docking in the N-terminal domain, which is distinguished from the well-known AHL-binding pocket (Lintz et al., 2011; Vannini et al., 2002; Zhang et al., 2007). Two pockets were adjacent to each other, and separated by five antiparallel  $\beta$ -sheets, the glucose-binding pocket located near the outer surface (Figure 3a,b). 3D models of the pocket indicated that the highly conserved structure may be essential for glucose binding (Figures 3a,b and 5a–e), although the LuxRs have relatively low amino acid sequence identities. Some PAB LuxR solos, such as XccR, XagR, and OryR (Chatnaparat et al., 2012; Ferluga & Venturi, 2009; Zhang et al., 2007), do not bind to canonical QS AHL compounds. Protein–ligand docking prediction provides us with information to gain insight into the architecture of ligand-binding sites, and amino acid substitution analysis confirmed the function of key residues of XccR. We found that three key residues of the XccR glucose-binding domain are important for maintaining a suitable structure for glucose embedding, Cys21, Tyr41, and Gln60, forming hydrogen bonds with glucose and stabilizing the complex conformation. Interestingly, the selected LuxRs showed structural conservation, and the number of hydrogen bonds between LuxR and glucose ranged from one to seven (Table S2). We deduced that the contribution of the key amino acids to the LuxR–glucose hydrogen bond formation is important for bacteria sensing glucose signals. It is possible that the LuxR glucose-binding pocket may also bind to other glucose structure-mimicking signals in nature. In addition, QscR and PsyR can respond to AHLs (Chatterjee et al., 2007; Fuqua, 2006) and bind to glucose in vitro; it is very likely that different signals are assigned to different pockets in the LuxR ligand-binding domain based on their hydrophobicity. These features of LuxRs may improve the ability of PABs to coordinately regulate their behaviours to adapt to the changing environment.

The *luxR* solo genes of PABs are usually in close proximity to the virulence *pip* genes (González & Venturi, 2013). The expression of *pip* is regulated by LuxR-like regulators through binding to the conserved inverted repeat DNA element (*lux* box) in the *pip* promoter,

which is important for several invading pathogens like Xcc, Xoo, and Xag (Chatnaparat et al., 2012; Ferluga & Venturi, 2009; Zhang et al., 2007). We proposed that XccR up-regulates *pip* expression through recruiting plant-derived glucose. Deletion of XccR or mutation of the key residues for binding glucose affected *gusA* expression driven by the *pip* promoter (in Xcc 8008) (Figure 4f), whereas the glucose concentration in plant tissues was similar after infection by Xcc wild-type and XccR mutant strains (data not shown). In *Atsweet* mutant plants, the reduced GUS activity in Xcc 8008 was restored by adding a certain amount of glucose (Figure 4e). Therefore, XccR may regulate *pip* expression depending on glucose recruitment in planta, which is beneficial for bacteria to coordinate virulence gene expression in host plants.

Our finding that glucose functions as a chemical signal extends the range of interkingdom signalling molecules. Exploration of how bacteria synchronize gene expression by monitoring or utilizing host chemical compounds is important to uncover the language and mechanisms of interkingdom communication. Our results indicate that these *luxR/pip* gene loci may constitute a new signalling system for plant signal perception that is representative of interkingdom signal circuits. Glucose can act in the pathogen either as a carbon source or as a direct signal that may be involved in the regulation of bacterial pathogenesis. Modulating or disrupting such interkingdom communication may offer effective approaches to control bacterial infection in plants.

## 4 | EXPERIMENTAL PROCEDURES

### 4.1 | Extraction and identification of effective plant compounds for XccR binding

Liquid nitrogen-frozen *Brassica oleracea* leaves were ground and then extracted with water. The aqueous extract was concentrated by a rotary evaporator and then passed through a 0.45- $\mu$ m filter, followed by ultrafiltration with a 1 kDa cut-off membrane (YM1; Amicon). The active fractions able to promote XccR binding to the *luxXc* box were identified by EMSA and then separated by Sephadex-G25 gel column chromatography eluting with gradient methanol–water solution. The active fraction was collected and subjected to HPLC profiling on an Asahipak NH2P-50 column eluted with gradient acetonitrile in water. The molecular weight of the chemical was determined by mass spectrometry and the structures were elucidated by  $^1\text{H}$  NMR at 500 MHz and  $^{13}\text{C}$  NMR at 126 MHz in deuterated methanol solution. The spectra were analysed using MestReNova (v. 6.1.0) software.

### 4.2 | Receptor–ligand binding prediction and validation

The prediction of protein structures was performed according to homologous structure templates in Protein Data Bank (PDB).

Sequence identity (SI) scores were calculated by comparing LuxR homologues to the respective templates, that is, template 3SZT\_A (SI = 24%) for XccR, 3SZT\_A (SI = 96%) for QscR, 3SZT\_A (SI = 31%) for PsyR, 1HOM\_A (SI = 27%) for OryR, 3SZT\_A (SI = 24%) for PsoR, 1HOM\_A (SI = 25%) for XagR, 3IX3\_A (SI = 100%) for LasR, and 1HOM\_A (SI = 98%) for TraR. 3D structures of these proteins were predicted using MODELLER (Webb & Sali, 2014). The docking ability of glucose in each putative pocket of LuxR was evaluated using Libdock (Diller & Merz, 2001) to identify putative glucose-binding pockets. Key amino acids forming hydrogen bonds with glucose were identified and graphed with Discovery Studio Visualizer.

Point mutations (C21A, Y41A, and Q60A) of XccR were generated using a site-directed fast mutagenesis system (Transgen Biotech). The MBP-tagged XccR and the mutated proteins were expressed in *Escherichia coli* TB1. The early log-phase culture of *E. coli* was induced overnight with 0.3 mM isopropyl- $\beta$ -D-thiogalactopyranoside at 16°C. The MBP fusion proteins were purified by affinity chromatography with amylose resin according to the procedure recommended by the manufacturer (New England Biolabs).

An Amicon Ultra-4 centrifugal filter device with a molecular weight cut-off of 10 kDa (Millipore) was used for protein concentration or buffer exchange. Protein purity was examined by SDS-PAGE followed by Coomassie blue staining.

### 4.3 | Phylogenetic analysis

LuxR protein sequences of different PABs were aligned using ClustalW. A phylogenetic tree was constructed with MEGA 7 (<http://www.megasoftware.net/>) using the neighbour-joining method with bootstrapping based on 1000 replicates.

### 4.4 | EMSA

EMSA were performed using MBP-tagged XccR and mutant proteins. The oligonucleotides containing the *luxXc* box sequence were annealed using the following primers: 46F (5'-AGATGCATGGCTAA CCTGGCAAATTTGCCAGTTATCCCGACCCGCT-3') and 46R (5'-AG CGGGTCGGGATAACTGGCAAATTTGCCAGGTTAGCCATGC-3'). Biotin was labelled at the 5' end of primer 46F, followed by annealing with primer 46R at 98°C for 10 min and a drop in temperature to produce biotin-labelled probe.

The DNA duplex was labelled using [ $\alpha$ -<sup>32</sup>P]-dATP (PerkinElmer) and the Klenow fragment of DNA polymerase I (Promega). Briefly, the reaction mixture (20  $\mu$ l) contained 2 nmol [<sup>32</sup>P]-labelled DNA duplex and different amounts of proteins and signal compounds (plant extract, glucose, sucrose, fructose, 2-deoxy-D-glucose, D-glucose 6-phosphate, and UDP-glucose) in a binding buffer of 10 mM Tris-HCl (pH 7.5), 50 mM KCl, 1 mM dithiothreitol (DTT), 2.5% glycerol, and 1  $\mu$ g poly(dI-dC), and was incubated for 20 min at room temperature. Samples were size-fractionated on a 6% native polyacrylamide

gel in 0.5 $\times$  Tris-borate-EDTA buffer at 4°C, and the [<sup>32</sup>P]-labelled probes were detected by a phosphor imaging system.

### 4.5 | Isothermal titration calorimetry assay

The binding affinity of glucose and XccR was measured using ITC (Sperandio et al., 2011) and MST (Panchal et al., 2016). Both the protein and glucose were prepared in phosphate-buffered saline (PBS) before titration, and all the solutions for titration were degassed under a vacuum prior to being loaded in the calorimeter. For each ITC measurement, a total of 25 injections of 10  $\mu$ l glucose were performed at intervals of 100 s under continuous stirring at 300 rpm. The protein was used at a concentration of 10  $\mu$ M in the microcalorimeter cell and glucose was injected at a concentration of 100  $\mu$ M, and the heat changes accompanying these additions were recorded. The titration experiment was repeated at least twice, and the data were calibrated with an MBP control and fitted with the one-site model to determine the binding constant ( $K_a$ ) using NanoAnalyze software from TA instruments.

### 4.6 | Microscale thermophoresis assay

The MST assay for protein-ligand interaction analysis was performed using a Monolith NT.115 instrument (Nanotemper Technologies). The protein was labelled with the RED fluorescent dye NT-647-NHS according to the procedure of the Monolith NT protein labelling kit. For each test, a titration series with constant receptor concentration (100 nM) and serial dilutions of ligand were prepared in a final solution of MST buffer (50 mM Tris-HCl, pH 7.4, 150 mM NaCl, 10 mM MgCl<sub>2</sub>, 0.05% Tween 20). The capillaries were filled with sample (less than 5  $\mu$ l for each capillary) and measured at 22°C using 20% LED power and 20% MST power. Laser on and off times were set at 30 and 5 s, respectively. The data were fitted to a  $K_d$  model and shown using Origin Pro. All experiments were conducted in triplicate.

### 4.7 | Pathogen inoculation and reverse transcription-quantitative PCR

*Arabidopsis* plants were inoculated with Xcc at a concentration of 10<sup>9</sup> cfu/ml with a needleless syringe, and the *AtSWEET* expression levels were measured at 8, 12, 24, and 36 h after inoculation by reverse transcription-quantitative PCR (RT-qPCR). Briefly, total RNA was isolated using a FastPure Cell/Tissue Total RNA Isolation Kit V2 (Vazyme; cat. no. RC112), and cDNA was synthesized using the *Evo M-MLV* RT Kit with gDNA Clean for qPCR (AG; cat. no. AG11705). qPCR was performed using a CFX96 Real-time System (Bio-Rad) with ChamQ Universal SYBR qPCR Master Mix (Vazyme; cat. no. Q711-02). *AtACTIN2* was used as the reference gene, and transcript levels of each *SWEET* gene were normalized to the levels in uninfected sample. Normalized RT-qPCR values are presented as

means  $\pm$  standard error of the mean (SEM) of three biological replicates. The primers used for RT-qPCR are listed in Table S3.

For the bacterial growth assay, Xcc was inoculated at a cell density of  $10^5$  cfu/ml with a needleless syringe into the leaves of wild-type Col-0 and *Atsweet* mutant plants. Bacterial populations were quantified at 2 dpi using the flat colony counting method. Necrosis on leaves was photographed at day 5 after pathogen inoculation.

#### 4.8 | Measurement of sugar levels

Apoplastic sugar concentrations of symmetrical locations on the same leaves challenged with  $10^6$  cfu/ml of bacteria or sterile water as control were measured at 3 dpi. Apoplastic fluids were extracted from the leaves by centrifugation (Roman-Reyna & Rathjen, 2017) and sugars were extracted in a two-step ethanol–water procedure using 50 mg of leaf material as described by Ikram et al. (2012). In the first step, the apoplastic fluids of leaves were extracted at 80°C using 500  $\mu$ l of 80% (vol/vol) ethanol for 25 min and centrifuged at 20,000  $\times$ g for 10 min. In the second step, the extraction was completed by using 500  $\mu$ l of water at 80°C for 20 min followed by centrifugation at 20,000  $\times$ g for 10 min. The above two supernatants were combined for further analyses of apoplastic sugar contents. The sugar contents were determined using an enzymatic assay with a commercial kit (Sucrose/D-glucose/D-fructose Assay Kit; Megazyme).

Xcc was cultured in MM (Daniels, Barber, Turner, Sawczyc, et al., 1984b) with glucose and harvested at OD<sub>600</sub> values of 0.1, 0.6, and 1.0. About  $10^{11}$  bacterial cells were collected by centrifugation, and the pellet was washed twice with PBS and resuspended in PBS. The suspended bacterial cells were crushed by high-pressure homogenization (French press), and the supernatant was used to measure the glucose concentration by the D-Glucose Content Assay Kit (GOPOD Format) (BOXBIO; cat. no. AKSU001M). To detect XccR-bound glucose, suspended bacterial cells were incubated with Dynabeads protein G (Invitrogen) bound with anti-XccR for at least 5 h in 4°C, and the supernatant glucose levels was measured by the D-Glucose Content Assay Kit. The amount of XccR-bound glucose was calculated as total glucose minus supernatant glucose.

#### 4.9 | Invertase activity assay

The invertase activity assay was performed as previously described (Wright et al., 1998). Apoplastic fluids were extracted from 50 mg of leaves and homogenized in 400  $\mu$ l extraction buffer (50 mM HEPES–KOH, 2 mM EDTA, 5 mM MgCl<sub>2</sub>, 1 mM MnCl<sub>2</sub>, 1 mM CaCl<sub>2</sub>, 1 mM DTT, 0.1 mM PMSF) and incubated on ice for 10 min. Samples were centrifuged at 13,000  $\times$ g for 10 min at 4°C. The pellet was washed twice with 400  $\mu$ l extraction buffer and centrifuged at 13,000  $\times$ g for 10 min at 4°C. The pellet was resolved in 400  $\mu$ l 50 mM sodium acetate buffer (pH 4.8) containing 0.1 M sucrose,

and the mixture was incubated at 37°C for 120 min. The reaction buffer without pellet served as the negative control. The activity of cell-wall invertase was determined by measuring the amount of glucose through the following steps. Glucose was phosphorylated to glucose 6-phosphate (G-6-P) by hexokinase, and then G-6-P was oxidized by NADP<sup>+</sup> to gluconate 6-phosphate with the formation of reduced NADPH. The increase in NADPH was measured by detecting the absorbance at 340 nm. The amount of NADPH formed in the reaction is stoichiometric with the amount of glucose (Hajirezaei et al., 2000).

#### 4.10 | Construction of bacterial mutants

The XccR null mutant was generated from Xcc 8008 (Xcc *pip-P/gusA* fusion strain) (Zhang et al., 2007). Briefly, two sequences (about 500 bp) upstream and downstream of the XccR-coding regions, respectively, were amplified by PCR. After digestion with appropriate enzymes, the two fragments were inserted into the vector pK18mobSacB to generate pK18xccR. The pK18xccR plasmid conferring kanamycin resistance (Kan<sup>R</sup>) and sucrose sensitivity (Suc<sup>S</sup>) was verified by restriction digestion and DNA sequencing and then transferred to Xcc 8008. Allelic replacement was achieved by sequential selection on kanamycin (100  $\mu$ g/ml) and 10% sucrose to create the XccR null mutant ( $\Delta$ XccR). The coding sequences of XccR or its variants from MBP-tagged protein expression strains were digested with *Bam*HI/*Hind*III, ligated to plasmid pLAFR3, and transferred to the XccR null mutant to obtain the complementary strains.

The *sglT* null mutant ( $\Delta$ *sglT*) was generated from Xcc 8008 (Xcc *pip-P/gusA* fusion strain). Two fragments (about 500 bp) upstream and downstream of the *sglT* coding regions were amplified by PCR and digested with *Eco*RI/*Hind*III, ligated to pK18mobSacB, and transferred to Xcc 8008, followed by screening by the above method to create the *sglT* null mutant ( $\Delta$ *sglT*). The promoter and coding sequences of *SglT* were digested with *Bam*HI/*Hind*III, ligated to plasmid pLAFR6, and transferred to the *sglT* null mutant to obtain the complementary strain.

#### 4.11 | Measurement of GUS activity

Bacterial cells were harvested from 200 ml NYG medium (Daniels, Barber, Turner, Cleary, & Sawczyc, 1984a) at OD<sub>600</sub> 1.0 and resuspended in sterile distilled water to an OD<sub>600</sub> of 0.1. *Arabidopsis* seedlings (4 weeks old) were infiltrated using this cell suspension with a needleless syringe, and GUS activities were assayed after 2 days and normalized according to the bacterial cell numbers as previously described (Zhang et al., 2007). One unit of enzyme activity is defined as the amount of enzyme that releases 1 pmol of 4-methylumbelliferone (MU) per min at pH 7.0 at 37°C. The experiments were repeated at least three times for each of the conditions, each time in biological triplicate.

## ACKNOWLEDGEMENTS

This work was supported by grants from the Strategic Priority Research Program of the Chinese Academy of Sciences (no. XDA28030000) and the National Natural Science Foundation of China (no. 31972233).

## DATA AVAILABILITY STATEMENT

The data that support the findings of this study are available from the corresponding author on reasonable request.

## ORCID

Li Wang  <https://orcid.org/0000-0001-5301-9897>

Xiu-Jie Wang  <https://orcid.org/0000-0001-7865-0204>

Rongxiang Fang  <https://orcid.org/0000-0002-1677-4591>

Yantao Jia  <https://orcid.org/0000-0001-8700-4271>

## REFERENCES

- Ahmer, B.M. (2004) Cell-to-cell signalling in *Escherichia coli* and *Salmonella enterica*. *Molecular Microbiology*, 52, 933–945.
- Bassler, B.L., Greenberg, E.P. & Stevens, A.M. (1997) Cross-species induction of luminescence in the quorum-sensing bacterium *Vibrio harveyi*. *Journal of Pathology and Bacteriology*, 179, 4043–4045.
- Berger, S., Sinha, A.K. & Roitsch, T. (2007) Plant physiology meets phytopathology: plant primary metabolism and plant-pathogen interactions. *Journal of Experimental Botany*, 58, 4019–4026.
- Bonfig, K.B., Gabler, A., Simon, U.K., Luschin-Ebengreuth, N., Hatz, M., Berger, S. et al. (2010) Post-translational derepression of invertase activity in source leaves via down-regulation of invertase inhibitor expression is part of the plant defense response. *Molecular Plant*, 3, 1037–1048.
- Bottomley, M.J., Muraglia, E., Bazzo, R. & Carfi, A. (2007) Molecular insights into quorum sensing in the human pathogen *Pseudomonas aeruginosa* from the structure of the virulence regulator LasR bound to its autoinducer. *Journal of Biological Chemistry*, 282, 13592–13600.
- Brencic, A. & Winans, S.C. (2005) Detection of and response to signals involved in host-microbe interactions by plant-associated bacteria. *Microbiology and Molecular Biology Reviews*, 69, 155–194.
- Case, R.J., Labbate, M. & Kjelleberg, S. (2008) AHL-driven quorum-sensing circuits: their frequency and function among the proteobacteria. *ISME Journal*, 2, 345–349.
- Cha, C., Gao, P., Chen, Y.C., Shaw, P.D. & Farrand, S.K. (1998) Production of acyl-homoserine lactone quorum-sensing signals by gram-negative plant-associated bacteria. *Molecular Plant-Microbe Interactions*, 11, 1119–1129.
- Chatnaparat, T., Prathuangwong, S., Ionescu, M. & Lindow, S.E. (2012) XagR, a LuxR homolog, contributes to the virulence of *Xanthomonas axonopodis* pv. *glycines* to soybean. *Molecular Plant-Microbe Interactions*, 25, 1104–1117.
- Chatterjee, A., Cui, Y., Hasegawa, H. & Chatterjee, A.K. (2007) PsrA, the *Pseudomonas* sigma regulator, controls regulators of epiphytic fitness, quorum-sensing signals, and plant interactions in *Pseudomonas syringae* pv. *tomato* strain DC3000. *Applied and Environmental Microbiology*, 73, 3684–3694.
- Chen, L.Q., Hou, B.H., Lalonde, S., Takanaga, H., Hartung, M.L., Qu, X.Q. et al. (2010) Sugar transporters for intercellular exchange and nutrition of pathogens. *Nature*, 468, 527–532.
- Chen, M., Bing, L. & Liu, J. (2014) Knock out deletion and functional analysis of glucose transportation system in *Xanthomonas campestris* pv. *campestris*. *Acta Agriculturae Zhejiangensis*, 26, 100–104.
- Chen, H.Y., Huh, J.H., Yu, Y.C., Ho, L.H., Chen, L.Q., Tholl, D. et al. (2015) The *Arabidopsis* vacuolar sugar transporter SWEET2 limits carbon sequestration from roots and restricts *Pythium* infection. *The Plant Journal*, 83, 1046–1058.
- Chen, L.Q., Cheung, L.S., Feng, L., Tanner, W. & Frommer, W.B. (2015) Transport of sugars. *Annual Review of Biochemistry*, 84, 865–894.
- Choi, S.H. & Greenberg, E.P. (1991) The C-terminal region of the *Vibrio fischeri* LuxR protein contains an inducer-independent lux gene activating domain. *Proceedings of the National Academy of Sciences of the United States of America*, 88, 11115–11119.
- Choi, S.H. & Greenberg, E.P. (1992) Genetic dissection of DNA-binding and luminescence gene activation by the *Vibrio fischeri* LuxR protein. *Journal of Bacteriology*, 174, 4064–4069.
- Corral-Lugo, A., Daddaoua, A., Ortega, A., Espinosa-Urgel, M. & Krell, T. (2016) Rosmarinic acid is a homoserine lactone mimic produced by plants that activates a bacterial quorum-sensing regulator. *Science Signaling*, 9, ra1.
- Daniels, M.J., Barber, C.E., Turner, P.C., Cleary, W.G. & Sawczyc, M.K. (1984) Isolation of mutants of *Xanthomonas campestris* pv. *campestris* showing altered pathogenicity. *Microbiology*, 130, 2447–2455.
- Daniels, M.J., Barber, C.E., Turner, P.C., Sawczyc, M.K., Byrde, R.J. & Fielding, A.H. (1984) Cloning of genes involved in pathogenicity of *Xanthomonas campestris* pv. *campestris* using the broad host range cosmid pLAFR1. *EMBO Journal*, 3, 3323–3328.
- Diller, D.J. & Merz, K.M., Jr. (2001) High throughput docking for library design and library prioritization. *Proteins*, 43, 113–124.
- Eom, J.S., Chen, L.Q., Sosso, D., Julius, B.T., Lin, I.W., Qu, X.Q. et al. (2015) SWEETs, transporters for intracellular and intercellular sugar translocation. *Current Opinion in Plant Biology*, 25, 53–62.
- Ferluga, S. & Venturi, V. (2009) OryR is a LuxR-family protein involved in interkingdom signaling between pathogenic *Xanthomonas oryzae* pv. *oryzae* and rice. *Journal of Pathology and Bacteriology*, 191, 890–897.
- Ferluga, S., Bigirimana, J., Hofte, M. & Venturi, V. (2007) A LuxR homologue of *Xanthomonas oryzae* pv. *oryzae* is required for optimal rice virulence. *Molecular Plant Pathology*, 8, 529–538.
- Fotopoulos, V., Gilbert, M.J., Pittman, J.K., Marvier, A.C., Buchanan, A.J., Sauer, N. et al. (2003) The monosaccharide transporter gene, *AtSTP4*, and the cell-wall invertase, *Atbfruct1*, are induced in *Arabidopsis* during infection with the fungal biotroph *Erysiphe cichoracearum*. *Plant Physiology*, 132, 821–829.
- Fuqua, C. (2006) The QscR quorum-sensing regulon of *Pseudomonas aeruginosa*: an orphan claims its identity. *Journal of Pathology and Bacteriology*, 188, 3169–3171.
- Fuqua, W.C., Winans, S.C. & Greenberg, E.P. (1994) Quorum sensing in bacteria: the LuxR-LuxI family of cell density-responsive transcriptional regulators. *Journal of Pathology and Bacteriology*, 176, 269–275.
- Fuqua, C., Parsek, M.R. & Greenberg, E.P. (2001) Regulation of gene expression by cell-to-cell communication: acyl-homoserine lactone quorum sensing. *Annual Review of Genetics*, 35, 439–468.
- González, J.F. & Venturi, V. (2013) A novel widespread interkingdom signaling circuit. *Trends in Plant Science*, 18, 167–174.
- Gorin, P.A. & Mazurek, M. (1975) Further studies on the assignment of signals in <sup>13</sup>C magnetic resonance spectra of aldoses and derived methyl glycosides. *Canadian Journal of Chemistry*, 53, 1212–1223.
- Hajirezaei, M.R., Takahata, Y., Trethewey, R.N., Willmitzer, L. & Sonnewald, U. (2000) Impact of elevated cytosolic and apoplastic invertase activity on carbon metabolism during potato tuber development. *Journal of Experimental Botany*, 51, 439–445.
- Horsfall, J.G. & Dimond, A.E. (1957) Interactions of tissue sugar, growth substances, and disease susceptibility. *Zeitschrift für Pflanzenkrankheiten (Pflanzenpathologie) und Pflanzenschutz*, 64, 415–421.
- Ikram, S., Bedu, M., Daniel-Vedele, F., Chaillou, S. & Chardon, F. (2012) Natural variation of *Arabidopsis* response to nitrogen availability. *Journal of Experimental Botany*, 63, 91–105.

- Keshavan, N.D., Chowdhary, P.K., Haines, D.C. & Gonzalez, J.E. (2005) L-canavanine made by *Medicago sativa* interferes with quorum sensing in *Sinorhizobium meliloti*. *Journal of Bacteriology*, 187, 8427–8436.
- Kocal, N., Sonnewald, U. & Sonnewald, S. (2008) Cell wall-bound invertase limits sucrose export and is involved in symptom development and inhibition of photosynthesis during compatible interaction between tomato and *Xanthomonas campestris* pv. *vesicatoria*. *Plant Physiology*, 148, 1523–1536.
- Kosaka, A., Aida, M. & Katsumoto, Y. (2015) Reconsidering the activation entropy for anomericization of glucose and mannose in water studied by NMR spectroscopy. *Journal of Molecular Structure*, 1093, 195–200.
- Lapin, D., Kovacova, V., Sun, X., Dongus, J.A., Bhandari, D., von Born, P. et al. (2019) A coevolved EDS1-SAG101-NRG1 module mediates cell death signaling by TIR-domain immune receptors. *The Plant Cell*, 31, 2430–2455.
- Lee, J.H., Lequette, Y. & Greenberg, E.P. (2006) Activity of purified QscR, a *Pseudomonas aeruginosa* orphan quorum-sensing transcription factor. *Molecular Microbiology*, 59, 602–609.
- Lintz, M.J., Oinuma, K., Wyszczynski, C.L., Greenberg, E.P. & Churchill, M.E. (2011) Crystal structure of QscR, a *Pseudomonas aeruginosa* quorum sensing signal receptor. *Proceedings of the National Academy of Sciences of the United States of America*, 108, 15763–15768.
- Lowery, C.A., Dickerson, T.J. & Janda, K.D. (2008) Interspecies and interkingdom communication mediated by bacterial quorum sensing. *Chemical Society Reviews*, 37, 1337–1346.
- Manefield, M., Rasmussen, T.B., Henzter, M., Andersen, J.B., Steinberg, P., Kjelleberg, S. et al. (2002) Halogenated furanones inhibit quorum sensing through accelerated LuxR turnover. *Microbiology*, 148, 1119–1127.
- Miller, M.B. & Bassler, B.L. (2001) Quorum sensing in bacteria. *Annual Review of Microbiology*, 55, 165–199.
- Panchal, S., Roy, D., Chitrakar, R., Price, L., Breitbach, Z.S., Armstrong, D.W. et al. (2016) Coronatine facilitates *Pseudomonas syringae* infection of *Arabidopsis* leaves at night. *Frontiers in Plant Science*, 7, 880.
- Patrick, J.W. (1989) Solute efflux from the host at plant microorganism interfaces. *Australian Journal of Plant Physiology*, 16, 53–67.
- Rahme, L.G., Ausubel, F.M., Cao, H., Drenkard, E., Goumnerov, B.C., Lau, G.W. et al. (2000) Plants and animals share functionally common bacterial virulence factors. *Proceedings of the National Academy of Sciences of the United States of America*, 97, 8815–8821.
- Roman-Reyna, V. & Rathjen, J.P. (2017) Apoplastic sugar extraction and quantification from wheat leaves infected with biotrophic fungi. *Methods in Molecular Biology*, 1659, 125–134.
- Ruan, Y.L. (2014) Sucrose metabolism: gateway to diverse carbon use and sugar signaling. *Annual Review of Plant Biology*, 65, 33–67.
- Seo, Y.S., Cho, J.-I., Lee, S.K., Ryu, H.S., Han, M., Hahn, T.R. et al. (2007) Current insights into the primary carbon flux that occurs in plants undergoing a defense response. *Plant Stress*, 1, 42–49.
- Shadel, G.S., Young, R. & Baldwin, T.O. (1990) Use of regulated cell lysis in a lethal genetic selection in *Escherichia coli*: identification of the autoinducer-binding region of the LuxR protein from *Vibrio fischeri* ATCC 7744. *Journal of Bacteriology*, 172, 3980–3987.
- Shiner, E.K., Rumbaugh, K.P. & Williams, S.C. (2005) Inter-kingdom signaling: deciphering the language of acyl homoserine lactones. *FEMS Microbiology Reviews*, 29, 935–947.
- Sperandio, V., Rasko, D.A., Moreira, C.G., Li, D.R., Reading, N.C., Ritchie, J.M. et al. (2011) Inter-kingdom chemical signaling in host–bacterial associations. *FEBS Journal*, 278, 35.
- Stachel, S.E., Messens, E., Van Montagu, M. & Zambryski, P. (1985) Identification of the signal molecules produced by wounded plant cells that activate T-DNA transfer in *Agrobacterium tumefaciens*. *Nature*, 318, 624–629.
- Subramoni, S. & Venturi, V. (2009) LuxR-family 'solos': bachelor sensors/regulators of signalling molecules. *Microbiology*, 155, 1377–1385.
- Subramoni, S., Gonzalez, J.F., Johnson, A., Pechy-Tarr, M., Rochat, L., Paulsen, I. et al. (2011) Bacterial subfamily of LuxR regulators that respond to plant compounds. *Applied and Environmental Microbiology*, 77, 4579–4588.
- Subramoni, S., Salcedo, D.V.F. & Suarez-Moreno, Z.R. (2015) A bioinformatic survey of distribution, conservation, and probable functions of LuxR solo regulators in bacteria. *Frontiers in Cellular and Infection Microbiology*, 5, 16.
- Sutton, P.N., Henry, M.J. & Hall, J.L. (1999) Glucose, and not sucrose, is transported from wheat to wheat powdery mildew. *Planta*, 208, 426–430.
- Tang, D.J., He, Y.Q., Feng, J.X., He, B.R., Jiang, B.L., Lu, G.T. et al. (2005) *Xanthomonas campestris* pv. *campestris* possesses a single gluconeogenic pathway that is required for virulence. *Journal of Bacteriology*, 187, 6231–6237.
- Tymowska-Lalanne, Z. & Kreis, M. (1998) Expression of the *Arabidopsis thaliana* invertase gene family. *Planta*, 207, 259–265.
- Vandeputte, O.M., Kienrebeogo, M., Rajaoanson, S., Diallo, B., Mol, A., El Jaziri, M. et al. (2010) Identification of catechin as one of the flavonoids from *Combretum albiflorum* bark extract that reduces the production of quorum-sensing-controlled virulence factors in *Pseudomonas aeruginosa* PAO1. *Applied and Environmental Microbiology*, 76, 243–253.
- Vannini, A., Volpari, C., Gargioli, C., Muraglia, E., Cortese, R., De Francesco, R. et al. (2002) The crystal structure of the quorum sensing protein TraR bound to its autoinducer and target DNA. *The EMBO Journal*, 21, 4393–4401.
- Venturi, V. & Fuqua, C. (2013) Chemical signaling between plants and plant-pathogenic bacteria. *Annual Review of Phytopathology*, 51, 17–37.
- Voegelé, R.T., Struck, C., Hahn, M. & Mendgen, K. (2001) The role of haustoria in sugar supply during infection of broad bean by the rust fungus *Uromyces fabae*. *Proceedings of the National Academy of Sciences of the United States of America*, 98, 8133–8138.
- Wang, L., Zhang, L., Geng, Y., Xi, W., Fang, R. & Jia, Y. (2011) XerR, a negative regulator of XccR in *Xanthomonas campestris* pv. *campestris*, relieves its repressor function in planta. *Cell Research*, 21, 1131–1142.
- Waters, C.M. & Bassler, B.L. (2005) Quorum sensing: cell-to-cell communication in bacteria. *Annual Review of Cell and Developmental Biology*, 21, 319–346.
- Webb, B. & Sali, A. (2014) Comparative protein structure modeling using MODELLER. *Current Protocols in Bioinformatics*, 47, 5 6 1–5 6 32.
- Whitehead, N.A., Barnard, A.M., Slater, H., Simpson, N.J. & Salmond, G.P. (2001) Quorum-sensing in gram-negative bacteria. *FEMS Microbiology Reviews*, 25, 365–404.
- Williams, P.H. (1980) Black rot: a continuing threat to world crucifers. *Plant Disease*, 64, 736–742.
- Wright, D.P., Read, D.J. & Scholes, J.D. (1998) Mycorrhizal sink strength influences whole plant carbon balance of *Trifolium repens* L. *Plant, Cell and Environment*, 21, 881–891.
- Yang, B., Sugio, A. & White, F.F. (2006) Os8N3 is a host disease-susceptibility gene for bacterial blight of rice. *Proceedings of the National Academy of Sciences of the United States of America*, 103, 10503–10508.
- Yoon, J., Cho, L.H., Tun, W., Jeon, J.S. & An, G. (2021) Sucrose signaling in higher plants. *Plant Science*, 302, 110703.
- Yu, Y., Streubel, J., Balzergue, S., Champion, A., Boch, J., Koebnik, R. et al. (2011) Colonization of rice leaf blades by an African strain of *Xanthomonas oryzae* pv. *oryzae* depends on a new TAL effector that induces the rice nodulin-3 Os11N3 gene. *Molecular Plant-Microbe Interactions*, 24, 1102–1113.
- Yuan, M. & Wang, S. (2013) Rice MtN3/saliva/SWEET family genes and their homologs in cellular organisms. *Molecular Plant*, 6, 665–674.
- Yuan, M., Zhao, J., Huang, R., Li, X., Xiao, J. & Wang, S. (2014) Rice MtN3/saliva/SWEET gene family: evolution, expression profiling, and sugar transport. *Journal of Integrative Plant Biology*, 56, 559–570.
- Zhang, R.-g., Pappas, T., Brace, J.L., Miller, P.C., Oulmassov, T., Molyneux, J.M. et al. (2002) Structure of a bacterial quorum-sensing

transcription factor complexed with pheromone and DNA. *Nature*, 417, 971–974.

Zhang, L., Jia, Y., Wang, L. & Fang, R. (2007) A proline iminopeptidase gene upregulated *in planta* by a LuxR homologue is essential for pathogenicity of *Xanthomonas campestris* pv. *campestris*. *Molecular Microbiology*, 65, 121–136.

#### SUPPORTING INFORMATION

Additional supporting information can be found online in the Supporting Information section at the end of this article.

**How to cite this article:** Zhang, S., Kan, J., Liu, X., Wu, Y., Zhang, M., Ou, J. et al. (2023) Phytopathogenic bacteria utilize host glucose as a signal to stimulate virulence through LuxR homologues. *Molecular Plant Pathology*, 24, 359–373. Available from: <https://doi.org/10.1111/mpp.13302>